

EBUS:

The Eastern Boundary Upwelling Systems: highly productive regions of the Atlantic and Pacific oceans supporting about 20% of the world fish catch. It is therefore essential to know about the processes and fluxes that affect the productivity in these regions [Chavez and Messié, 2009].

Eddy-Driven Offshore Transport:

Eddies formed near-shore capture water and travel westward. This induces a net transport of mass and energy that does not follow main circulation patterns. It is known that this offshore transport of nutrients can inhibit primary production in the EBUS [Gruber et al., 2011].

Implications of Refined Altimetry:

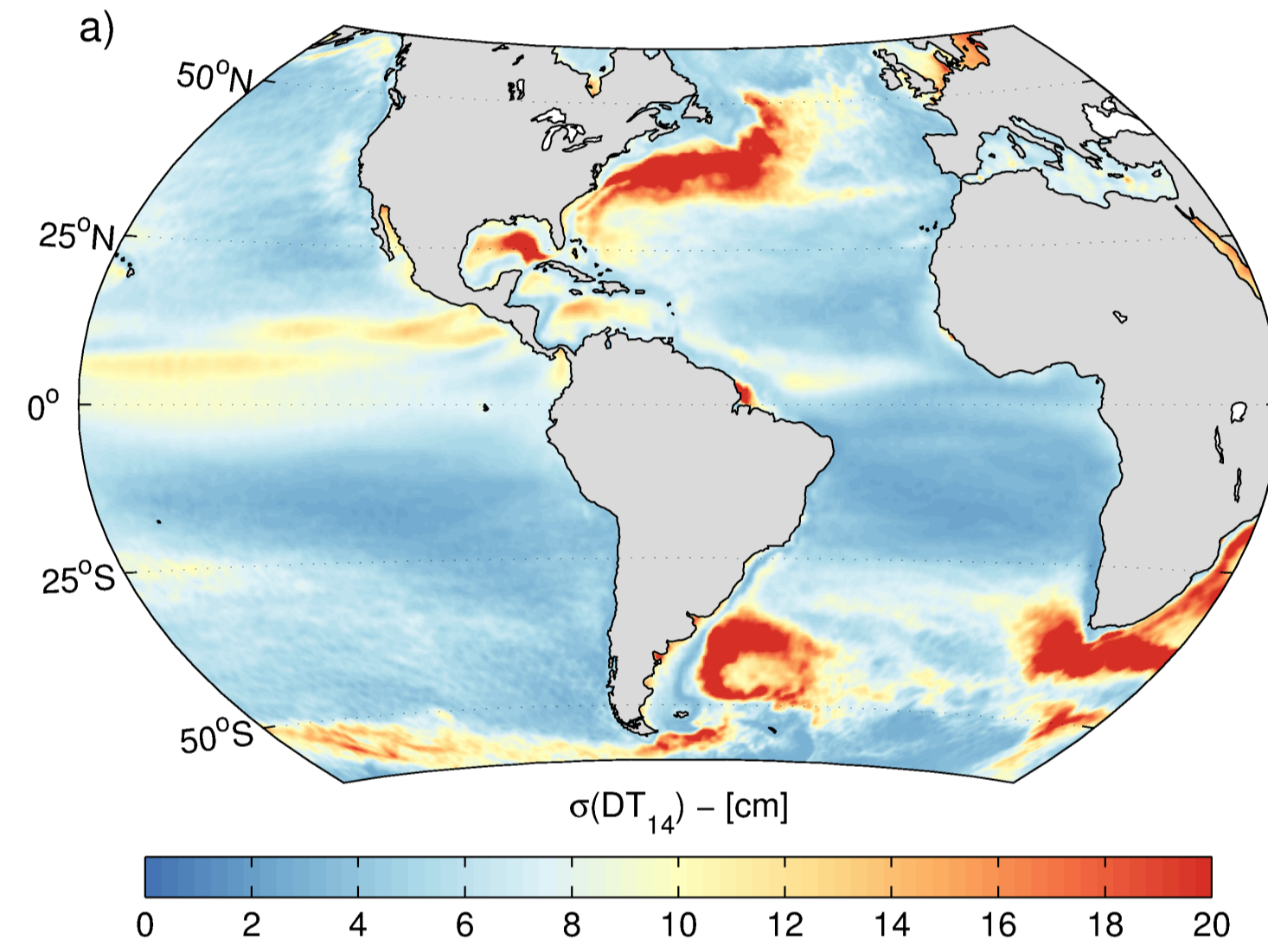
Eddies are identified through satellite altimetry. Refined altimetry products thus affect estimates of eddy-induced transport. We investigate how.

The revised AVISO altimeter dataset depicts higher mesoscale activity

After 20 years of observations the AVISO center went through a complete reprocessing of the Ssalto/Duacs sea level anomaly dataset. We compare the former gridded products **DT10** to the revised **DT14**, which is interpolated on a finer grid (1/4° Cartesian grid versus 1/3° Mercator grid) using refined correlation length scales and less filtered along-track data.

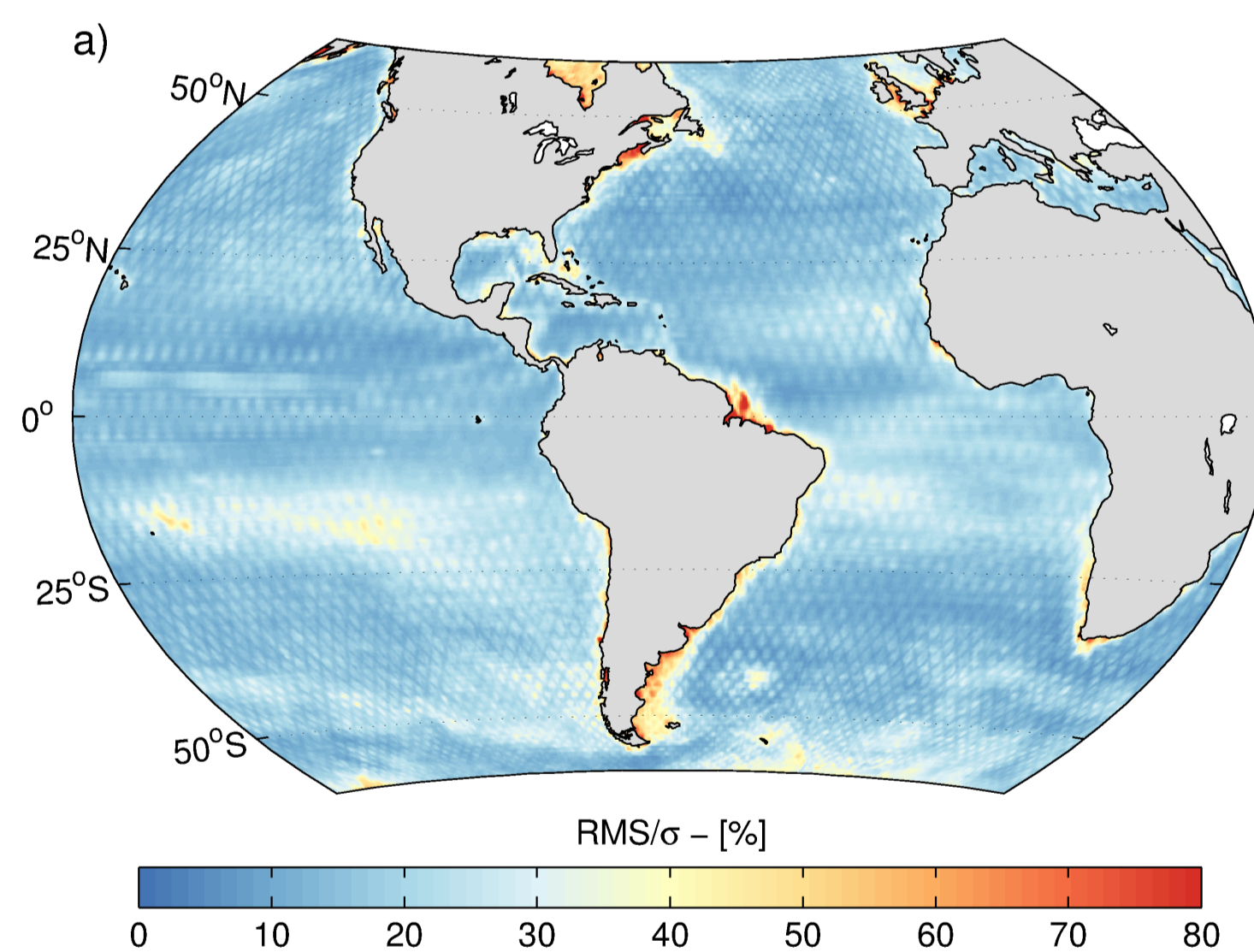
$$STD = \sqrt{\langle (DT_{14} - \langle DT_{14} \rangle)^2 \rangle}$$

The temporal standard deviation of sea level anomalies (SLA) evidences the regions of the world ocean where mesoscale activity is particularly important



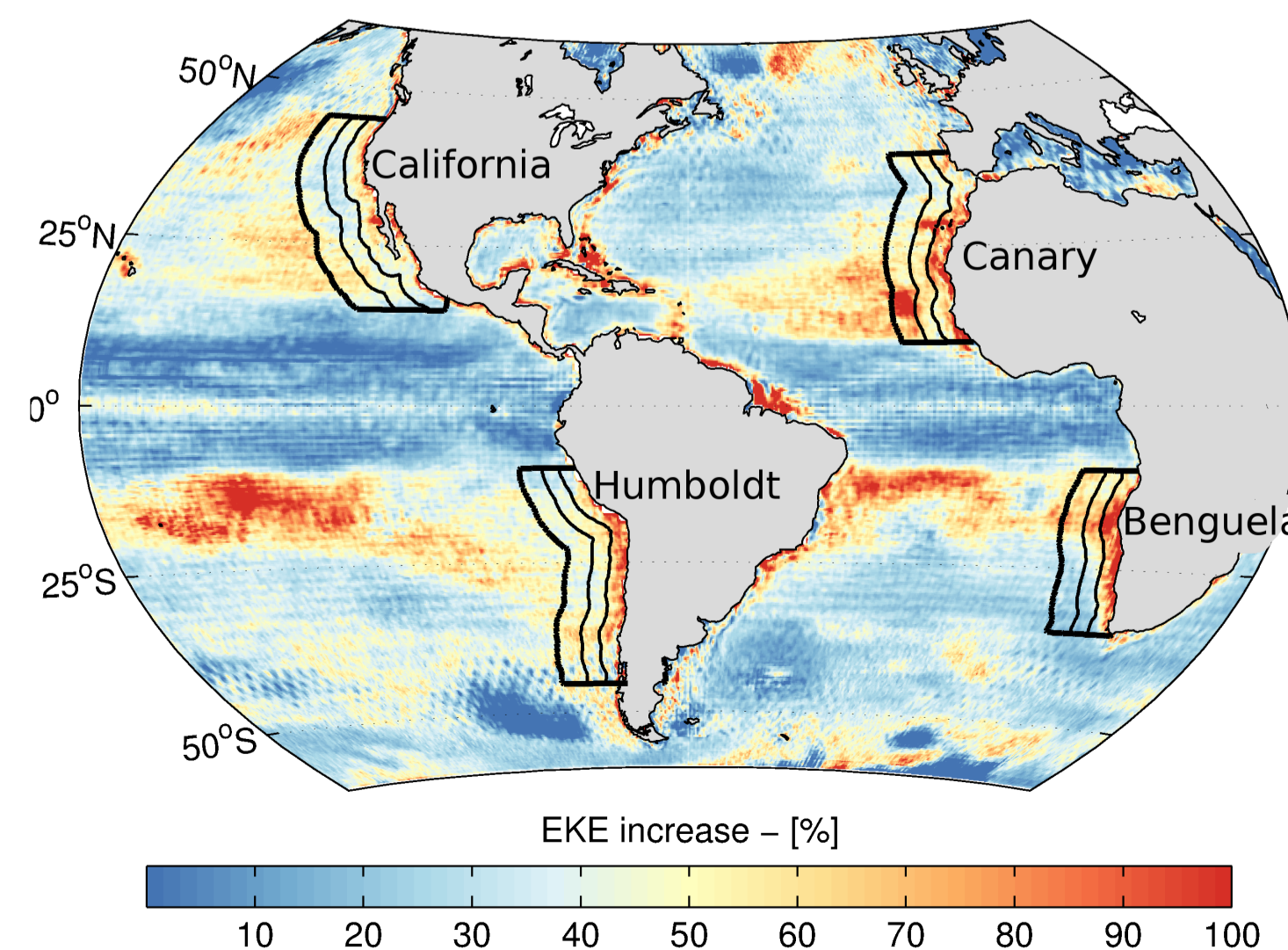
$$RMS/\sigma = \frac{\sqrt{\langle (DT_{14} - DT_{10})^2 \rangle}}{\sqrt{\langle (DT_{14} - \langle DT_{14} \rangle)^2 \rangle}}$$

The root mean square difference between **DT10** and **DT14** shows where the revised altimetric processing has had the most impact. Normalizing it by the STD shown above evidences the relative increase of SLA variations.



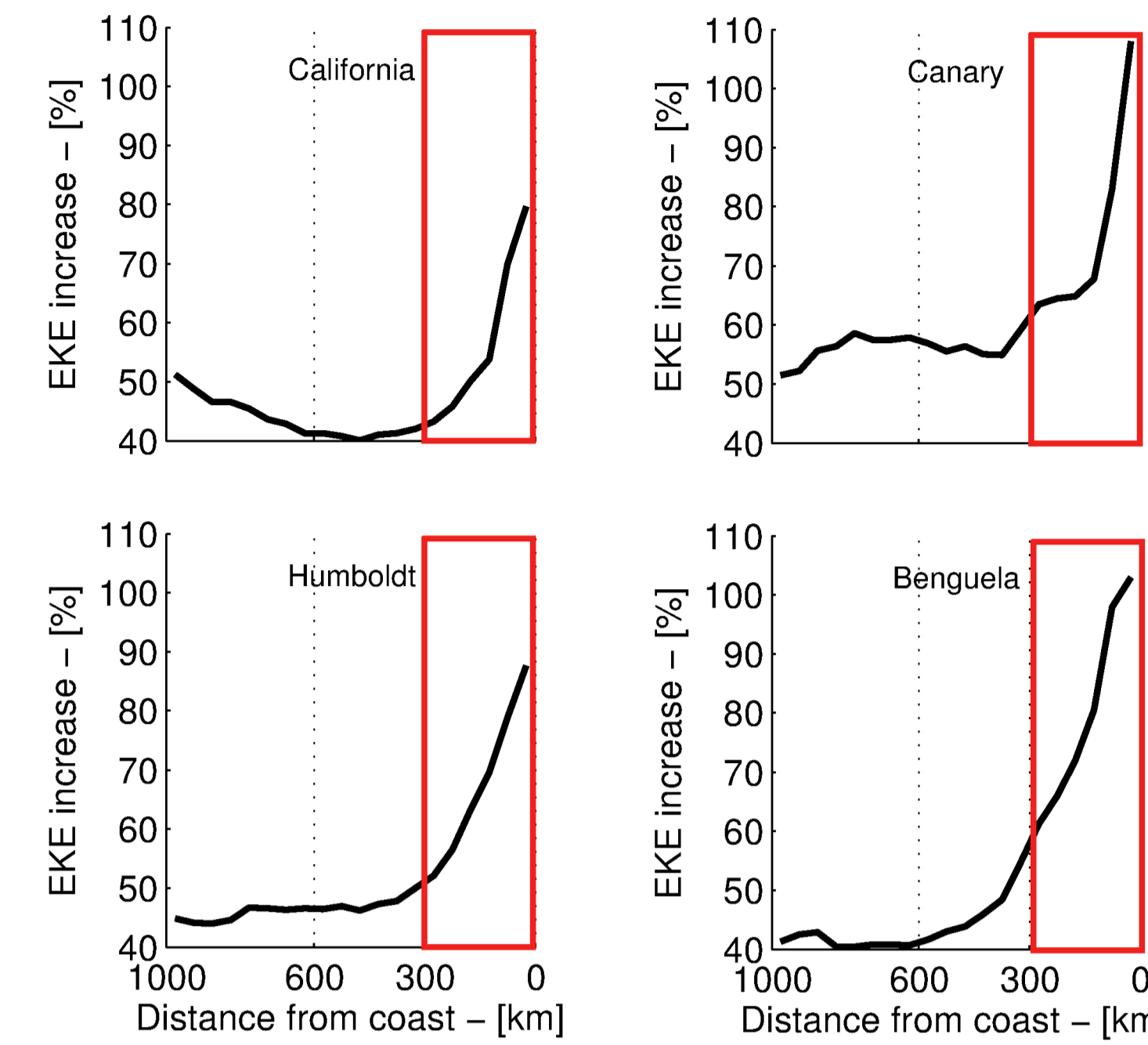
$$EKE = \frac{u'^2 + v'^2}{2}; EKE_{inc.} = \frac{EKE_{14} - EKE_{10}}{EKE_{10}}$$

u' and v' are the geostrophic velocities derived from sea level anomalies. The Eddy Kinetic Energy (EKE) therefore represents the kinetic energy contained in mesoscale motions, in opposition to the mean kinetic energy contained in large-scale circulation features. Because it resolves finer scales, **DT14** provides higher EKE values.



The higher mesoscale activity matches with in situ observations

Here we plot $EKE_{increase}$ just as in the last figure, but specifically for each EBUS, and expressed as a function of distance from the coast. What the figure tells us is that **DT14** really shows a higher mesoscale activity in the nearshore region of the EBUS. Now the question is: **Is that increase an improvement?**

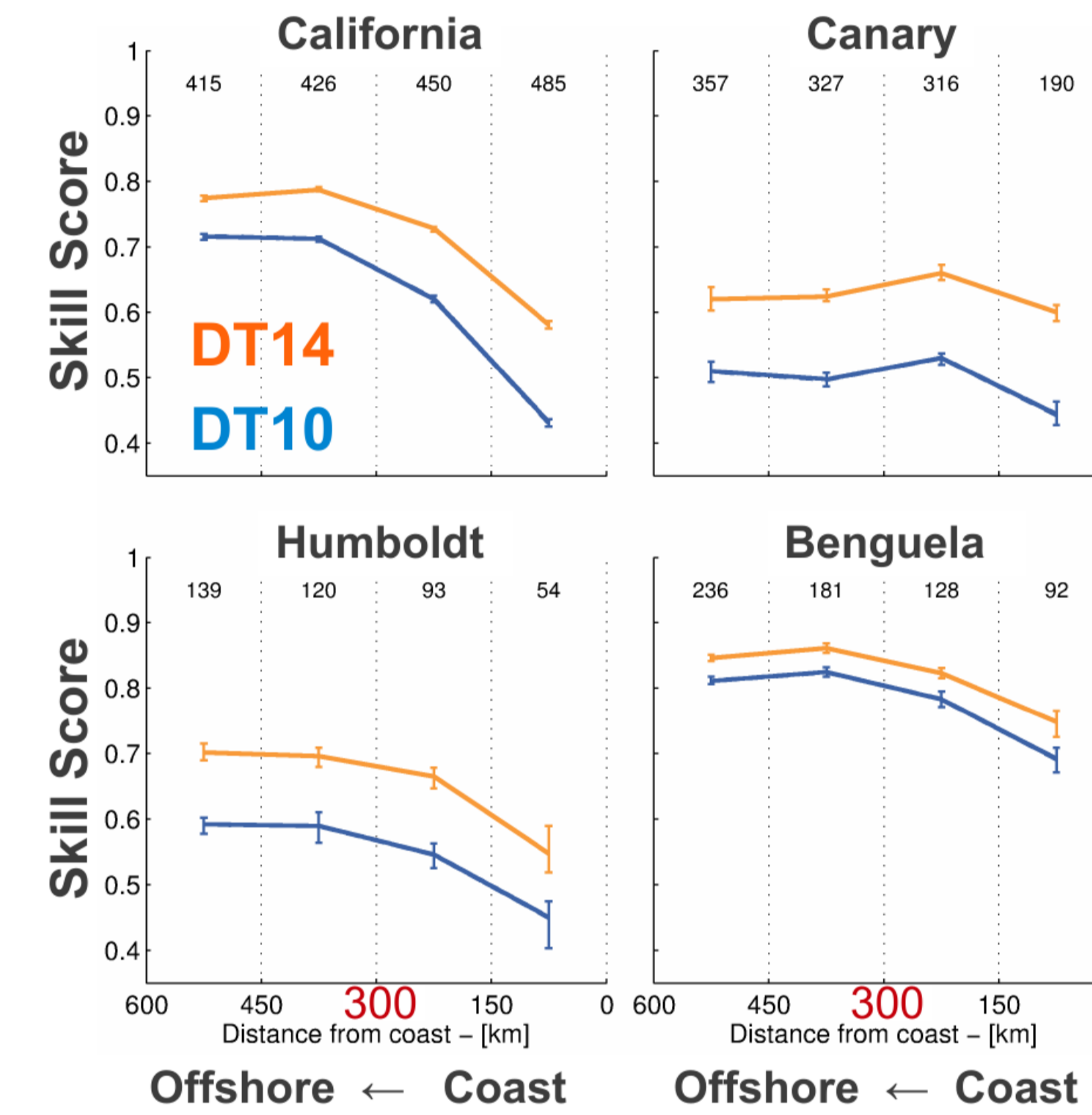


We compare the geostrophic velocities derived from **DT14** (absolute dynamic topography) with those interpreted from in-situ drifters (wind drift and Ekman corrected), and quantify the match using the Taylor Skill Score S ($S = 1 \rightarrow$ perfect match; $S = 0 \rightarrow$ no match).

$$S = \frac{4(1+R)}{2(\frac{\sigma_{sat}}{\sigma_{drift}} + \frac{\sigma_{drift}}{\sigma_{sat}})^2}$$

The comparison shows that

- The score decreases near shore
- The score is increased when using **DT14**
- The enhancement is marked in the nearshore regions of the EBUS



Eddy tracking and offshore transport estimates

The *py-eddy-tracker* algorithm [Mason et al., 2014] uses altimetry to provide tracks and sizes of drifting eddies. To quantify the resulting export (in terms of water volume), we simply sum the individual volumes (V_i) of westward-moving eddies crossing the 300 km cross-shore distance line.

$$Q = \frac{1}{T} \sum_{i=1}^n V_i$$

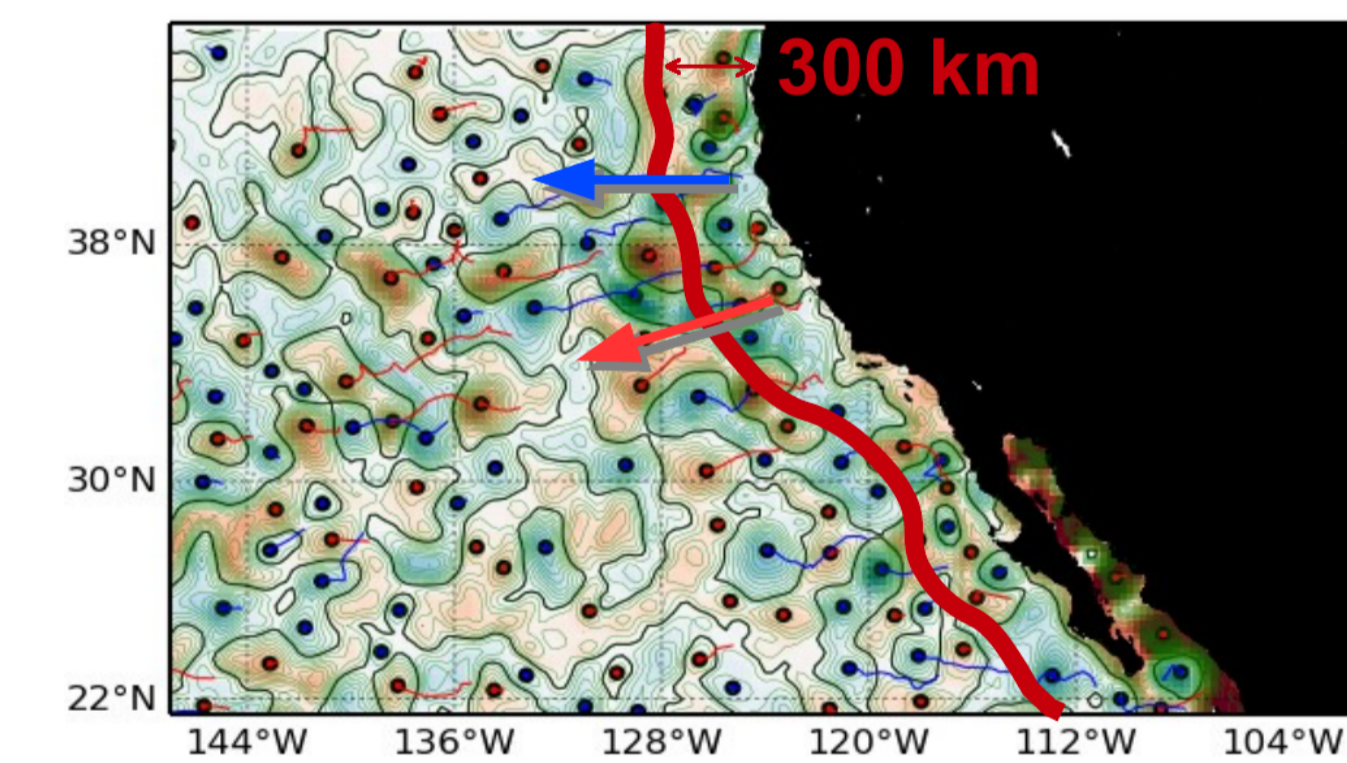
Estimating individual eddy volumes requires information about their vertical structure that can't be obtained from satellite. However, if we assume (1) that eddy volume has axial symmetry, and (2) that the vertical shape can be estimated independently from the radial extent, we can estimate (3) the relative increase in Q resulting from the use of **DT14** altimetry.

$$V = \pi \int [R(z)]^2 dz \quad (1)$$

$$R(z) = r \cdot H(z) \quad (2)$$

$R(z)$: distance, at depth z , between the outer limit of the eddy core and the central axis.

$H(z)$: an independent function giving the vertical shape of the eddy core.



$$\frac{Q_{14}}{Q_{10}} = \frac{\sum_{i=1}^{n_{14}} r_{14,i}^2}{\sum_{i=1}^{n_{10}} r_{10,i}^2} \quad (3)$$

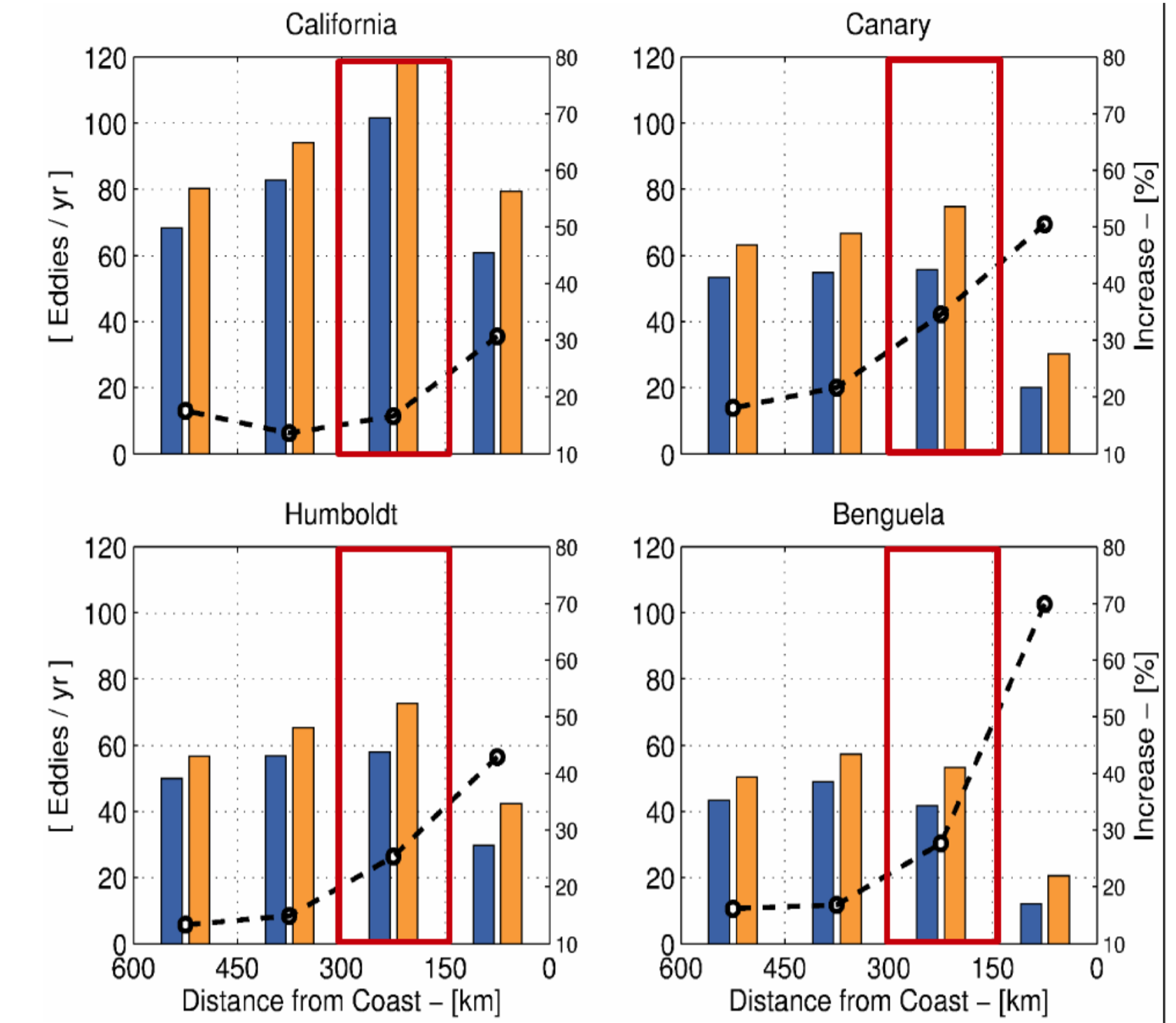
$n_{14}, r_{14,i}$: number of eddies and specific radii estimated using **DT14**

$n_{10}, r_{10,i}$: number of eddies and specific radii estimated using **DT10**

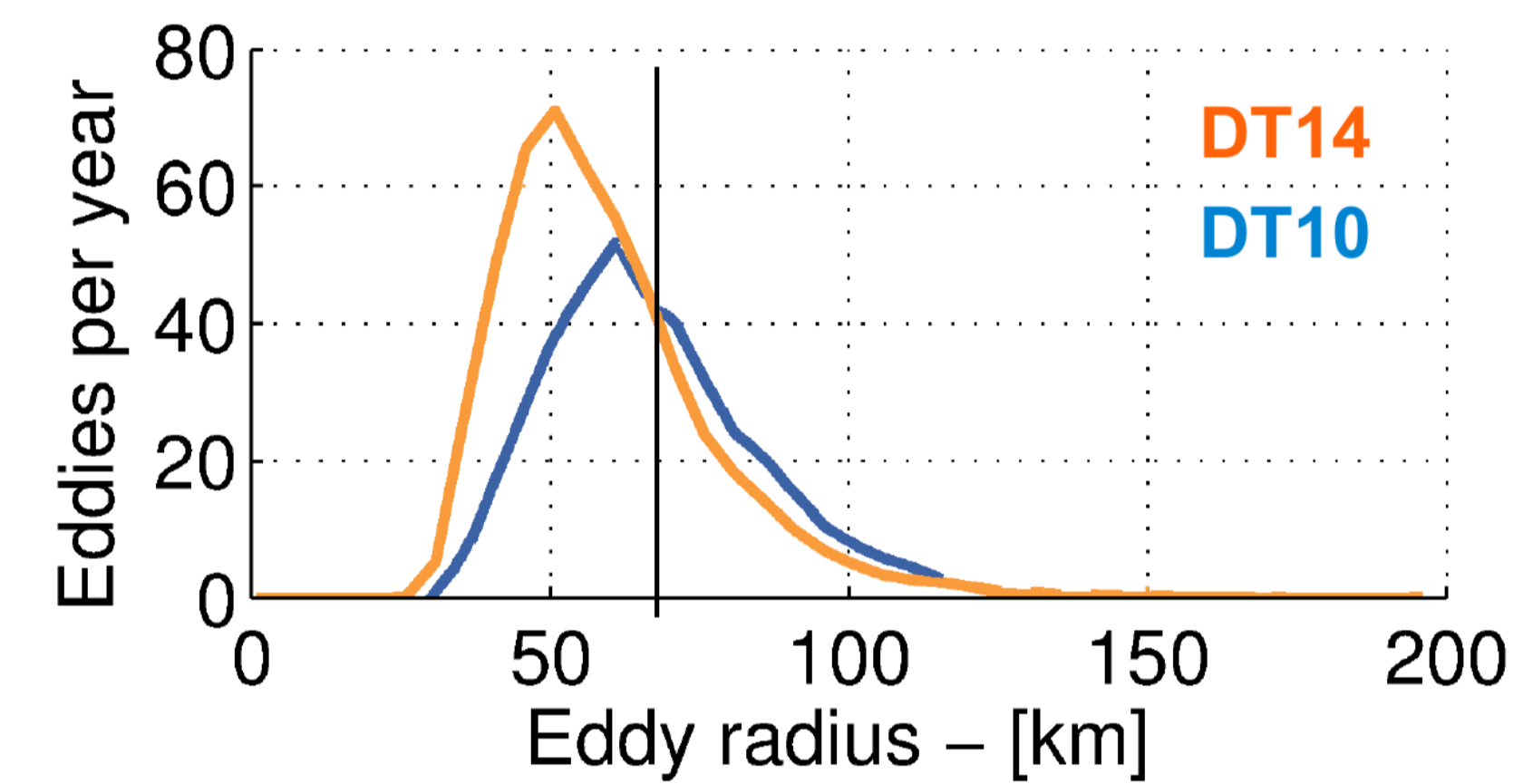
Using the revised altimetry reveals more eddies, with smaller radii

These figures compare the output of eddy-tracking applied on **DT10** and **DT14** sea level anomalies.

- The highest eddy density are obtained within 300km from the coast.
- More eddies are identified when using **DT14**.
- This increase is mostly marked near shore.



Sharper gradients in **DT14** \rightarrow Eddy tracking identifies more small eddies and less large eddies.



Conclusion

The revised altimetry products enhance the description of mesoscale activity in the nearshore regions of EBUS, which appeals for a reassessment of the relationship between mesoscale activity and primary production in the EBUS.

Smaller eddy radii obtained from AVISO 2014 altimetry leads to smaller transport estimates, despite the fact that more eddies were identified. The correlation length scales used in the mapping of along track altimetry affects global eddy transport estimates.

Rough estimates of net eddy-driven offshore transport from the EBUS 300 km coastal band can be obtained by considering semi-ellipsoidal eddies with vertical extents of 200-600 m.

	California	Canary	Humboldt	Benguela	Average
Increase in eddy density n_{14}/n_{10}	+8.5%	+18.2%	+11.1%	+11.8%	+12.4%
Increase in transport Q_{14}/Q_{10}	-13.8%	-10.5%	-16.1%	-9.6%	-12.5%
Transport estimates Q_{14} [Sv]	[5.0 – 14.9]	[2.8 – 8.5]	[4.3 – 13.1]	[3.6 – 10.9]	

References

- Chavez, F. P., and M. Messié (2009), *Progr Oceanogr*, 83(1), 80–96.
 Gruber, N., Z. Lachkar, H. Frenzel, P. Marchesiello, M. Münnich, J. C. McWilliams, T. Nagai, and G.-K. Plattner (2011), *Nature Geosci*, 4(11), 787–792.
 Mason, E., A. Pascual, and J. C. McWilliams (2014), *J Atmos Ocean Tech*, 31(5), 1181–1188.

Acknowledgements

This study was funded by the EU MyOcean2 project (EU N° FP7-SPA.2011.1.5-01-Grant Agreement 283367) Altimeter products are produced by SSALTO/DUACS and distributed by AVISO. V.R. acknowledges support from MICINN and FEDER through the ESCOLA project (CTM2012-39025-C02-01). E.M. is supported by a post-doctoral grant from the Conselleria d'Educació, Cultura i Universitats del Govern de les Illes Balears (Mallorca, Spain) and the European Social Fund.